
Methodologies for the comparison of gear measurement results using tactile and fibre optic laser interferometry sensors within a Coordinate measuring machine

Denis Sexton¹, Andy Sharpe², Robert Frazer³, Sofia Catalucci¹, Samanta Piano¹

¹Manufacturing Metrology Team, Faculty of Engineering, University of Nottingham, UK

²Department of Metrology and NDT, Manufacturing Technology Centre (MTC), UK

³National Gear Metrology Laboratory (NGML) Department of Engineering, Newcastle University, UK

denis.sexton@nottingham.ac.uk

Abstract

The growth of optical measurement techniques in recent years has introduced the possibility of allowing several alternative methods of non-contact gear measurement to be utilised. Optical methods offer many advantages over tactile ones such as the potential to evaluate delicate surfaces quickly and to measure the whole area of the gear tooth flank at the sub-micron level. However, in order to maximise this potential, the magnitude of error and sources of uncertainty need to be better understood. In order to allow greater confidence in the results obtained from optical measurements, a series of trials was undertaken with a known size artefact. This paper presents results obtained from the Hexagon HP-O optical measurement system when used in conjunction with traditional tactile probing for gear measurement. The use of a series of designed experiments (DOE/DOX) allowed deliberate changes to specific key instrument parameters to be explored. The results presented in this paper are intended as preliminary outcomes of the application of designed experiments as a tool to explore the cause-and-effect influence on predetermined instrument variables. Future work will include experiment campaigns and analysis, planned specifically to further validate the results obtained from the application of the proposed method. The planned gear measurement validation activities will be supported by the UK National Gear Metrology Laboratory (NGML).

Keywords: Optical Gear Metrology, Laser Interferometry, Analysis of Means, Analysis of Range, Orthogonal Array,

1. Introduction

Gear geometry as defined in ISO 1328-1:2013 [1] requires specific elements of the gear (i.e. profile, lead or helix, and pitch) to be considered independently. This ISO standard is used in conjunction with ISO TS 10064-1 [2] which defines approved gear inspection methods. Since the standard does not currently establish any optical technology methodologies to measure gears, these methods remain essentially tactile. Modern optical methods can offer many advantages over tactile, such as the ability to quickly measure the whole area of the gear tooth flank at the sub-micron level. Data extracted may then be used as a predictor model to aid gear design and wear analysis. BS ISO 18653:2003 [3] addresses gear traceability, calibration intervals, and sources of measurement error and uncertainties including mechanical alignment and drift. In order to explore the capabilities of optical techniques for gear measurement, one optical methodology was chosen. Measurement trials were performed to evaluate measurement results against a known size artefact, which in this case was a master gear provided by the UK National Gear Metrology Laboratory (NGML). The information gathered from these measurement trials could assist in defining the highest class of gear which could be evaluated utilising any given optical technology under predetermined conditions. Investigation may provide working models to explore error and uncertainty in other optical measurement systems. It may also be possible to obtain and provide useful information when defining any optical gear instrument suitability with reference to measuring multiple gear features against any specific tolerance classification. One

advantage offered by these trials, is that since both sensors exist within the same coordinate measuring machine (CMM) tool rack, any component alignment errors accumulated when moving between instruments are removed. Results from both sensors can also be evaluated directly in real time via Quindos® gear software.

2. Methodology and Gear Setup

A series of trials were planned for a NGML supplied spur gear on a Leitz PMM-C CMM at the MTC. The first series of trials were designed to look at the repeatability of the HPOAL-0010L optical sensor (as shown in Fig 1). In order to set a baseline, the gear was first aligned and measured twice with a conventional tactile ruby sphere of 3 mm diameter [4, 5]. Initial repeatability studies were made with the tactile sensor without the use of the rotary axis, while further tactile run included it. The profile scan speed was set at 2 mm/second with a distance of 0.005 mm between points, while the lead was scanned at 1 mm/second with a maximum distance of 0.0005 mm between points. The order of tooth scan was kept as left flank profile, then left flank lead, then right flank profile followed by right flank lead. Four of the teeth were scanned for each trial of profile and lead, and numbered as 1, 8, 16, and 23. Each sensor was utilised in a single orientation (tactile probe A axis = 0°, B axis = 0° and optical probe A axis = 90°, B axis = 0°). The rotary axis was utilised for all the trials, since it is not possible to utilise the optical sensor without the rotary axis due to indexing head constraints. Due to further constraints with the HPOAL optical sensor, a tactile versus optical comparison was not initially possible for the full depth of the tooth. Profile measurements were taken from the gear

reference diameter (equal to 113.10 mm) to the tip diameter (equal to 120.90 mm). The width of the teeth was 20 mm so an evaluation range of 14 mm was initially chosen for lead measurement, allowing 3 mm of clearance at each end of the tooth flanks. Following successful repeatability trials for both tactile and optical methods, the second phase of the experiments involving the optical scans was undertaken. In this paper the data obtained from the second phase of optical trials is reported.

2.1. Reportable features

The measurement results provided from the CMM gear software consists of various outputs, including those specific gear characteristics which are defined as mandatory reportable features [1]. These include profile (FH α), lead (FH β), individual pitch (fpi), cumulative pitch (Fpi) and runout (Fri). Profile and lead measurements are completed on both flanks of four of the total (29) teeth as previously identified, and at approximately 90 degrees apart. Individual and cumulative pitch are normally measured across both flanks of all teeth. Runout can be calculated from pitch measurements back to the defined datum axis [1]. Since it was not initially possible to scan the full length of each gear tooth due to specific optical hardware issues, the first trials were planned as a comparison between tactile CMM scanning and the HP-O optical scanning over the same tooth area. Individual pitch error (fpi) on one flank of the spur gear is reported in this paper. The methodology defined here is planned for further tactile and optical measurement studies.

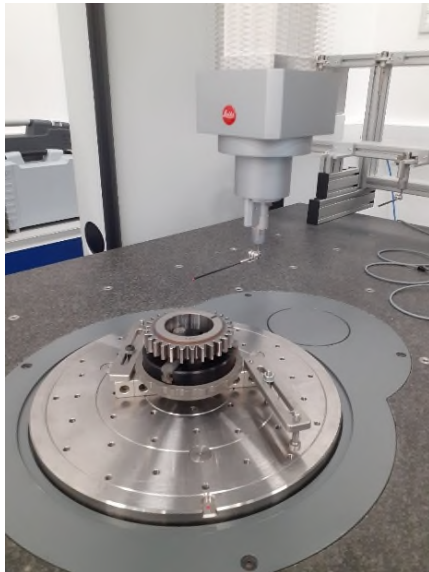


Fig 1. NGML Spur gear measured with the Hexagon HP-O (HPOAL) sensor on a Leitz PMM-C CMM at the MTC

3. Utilising ANOM and ANOR experimental control charts

When we are interested in repeatability (data recorded in time series under the same input settings), we can make use of statistical process control (SPC) charts such as the X -mR chart [6]. However, when we are looking at experimental data, we make use of a particular pair of SPC charts called Analysis of means (ANOM) and Analysis of Range (ANOR) [7]. The detection limits on ANOM & ANOR charts initially look similar to the control limits on a X-mR chart, but they differ slightly. SPC charts are used for data which is characterised by routine. On the other hand, experimental data is characterised by uniqueness. This is why control charts have a potential shortcoming as a tool for analysing experimental data. Industrial experiments will

generally involve the exploratory analysis of a limited amount of data that is, *a priori*, thought to contain real differences. Control charts are set up for the analysis of ongoing streams of data that hopefully contain no real differences. So, if a control chart is used to analyse experimental data, those differences identified as potential signals by the control chart are likely to represent real effects, though some real differences may be missed. In conclusion, the ANOM is different from the control chart for subgroup averages in two physical aspects: (a) ANOM is limited to a finite number of subgroups, and (b) ANOM requires the specification of an overall alpha level for the procedure (in this case 0.1 or 10% for ANOM, and 0.05 or 5% for the ANOR). The first of these differences prevents one from using the ANOM technique with production data. The second of these differences lets the user adjust the sensitivity of the ANOM procedure. ANOM tests whether the treatment means differ from the overall mean (also called the grand average) as will be shown.

3.1. Investigating the instrument variables on a test gear

The maximum individual pitch error (fpi) from the left flanks of a 29 tooth spur gear with a normal module of 3.9 were measured three times on the CMM. The measurements were recorded at two different point densities and at five different scan speeds to evaluate the effects of these changes as observed upon the results. The recorded results were gathered in a randomised fashion and are reported in Table 1 below.

Table 1. Experimental Trial Data

| Run Order # | Blocks | Point Density | Scan Speed | fpi (μm) |
|-------------|--------|---------------|------------|-----------------------|
| 1 | 1 | B | 1 | 3 |
| 2 | 1 | B | 2 | 3.5 |
| 3 | 1 | A | 1 | 1.9 |
| 4 | 1 | A | 5 | 3.5 |
| 5 | 1 | B | 5 | 3.8 |
| 6 | 1 | A | 3 | 3 |
| 7 | 1 | B | 3 | 3.9 |
| 8 | 1 | A | 4 | 3.1 |
| 9 | 1 | B | 4 | 3.6 |
| 10 | 1 | A | 2 | 2.8 |
| 11 | 2 | B | 3 | 3.2 |
| 12 | 2 | B | 2 | 4.7 |
| 13 | 2 | A | 1 | 1.8 |
| 14 | 2 | A | 2 | 2 |
| 15 | 2 | B | 5 | 4.6 |
| 16 | 2 | A | 5 | 3.9 |
| 17 | 2 | A | 3 | 3.1 |
| 18 | 2 | B | 4 | 4.4 |
| 19 | 2 | B | 1 | 3.8 |
| 20 | 2 | A | 4 | 3.7 |
| 21 | 3 | B | 4 | 3.9 |
| 22 | 3 | A | 4 | 3.6 |
| 23 | 3 | A | 3 | 3.3 |
| 24 | 3 | A | 5 | 3.6 |
| 25 | 3 | B | 3 | 3.8 |
| 26 | 3 | B | 1 | 3.1 |
| 27 | 3 | B | 2 | 4 |
| 28 | 3 | A | 2 | 2.3 |
| 29 | 3 | B | 5 | 4.1 |
| 30 | 3 | A | 1 | 2.2 |

3.2. Constructing the ANOM & ANOR charts

A set of three measurements were recorded for each of the ten combinations of point density and scan speed. The first variable, point density, has two levels coded as A and B (where A is higher density), while the second variable, scan speed, had five levels coded as 1,2,3,4, and 5 (where level 5 is fastest). Three questions can be asked:

1. How does the point density affect the results?
2. How does the scan speed affect the results?
3. Does any interaction exist between point density and scan speed (and is it statistically significant)?

Firstly, the data from Table 1 is plotted onto the ANOM control chart as shown in Fig 2. This process is similar to a conventional statistical process control chart, but the constants used for calculating the control limits and the terminology are slightly different. The detection limits are computed in a similar way to the control limits for the individual (X) and moving range (mR) chart. The grand average for all the data in the table is 3.373 μm and the average range is 0.68 μm . With an overall alpha level of 10 percent, the ANOM scaling factor (taken from ANOM statistical tables) for $k = 10$ subgroups of size $n = 3$ is 0.893. The ANOM detection limits in microns are calculated thus:

ANOM Detection Limits (LDL & UDL) =

$$\text{Grand Average} \pm \text{ANOM}_{.10} (\text{Average Range}) \quad (1)$$

$$= 3.373 \mu\text{m} \pm 0.893 (0.68) = 2.766 \mu\text{m} (\text{LDL}) \text{ and } 3.981 \mu\text{m} (\text{UDL})$$

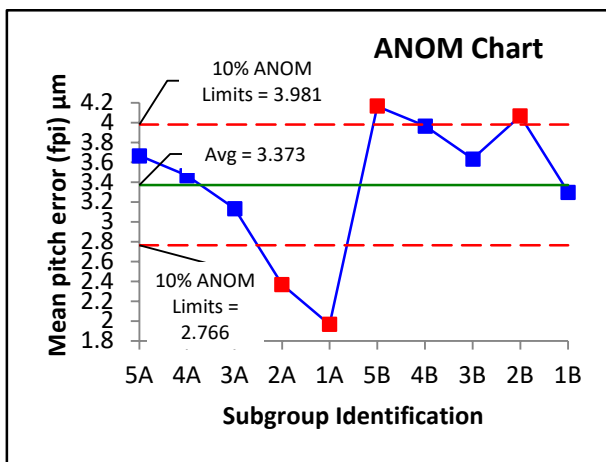


Fig 2. ANOM Chart constructed from data in Table 1

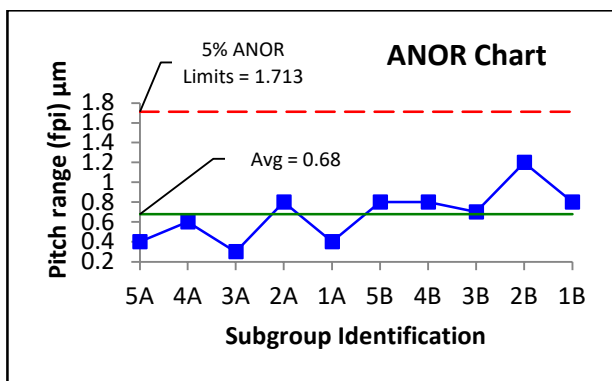


Fig 3. ANOR Chart constructed from data in Table 1

The analysis of ranges (ANOR) proceeds in a similar manner as shown in Fig 3. With an alpha level of 5 percent, and with $k = 10$ and $n = 3$, the ANOR scaling factor (taken from ANOR statistical

tables) for $k = 10$ subgroups of size $n = 3$ is 2.519. The ANOR detection limits are then calculated thus:

ANOR Upper Detection Limit (UDL) =

$$\text{ANOR}_{.05} (\text{Average Range}) \quad (2)$$

$$\text{UDL} = 2.519 (0.68) = 1.713 \mu\text{m}$$

There is no lower detection limit (LDL) for this ANOR chart.

3.3. Observations

From the range (ANOR) chart it is possible to observe that each group has similar “within group” variation. Additionally, it can be seen that the point density is significant, as it is shown in the “between group” means (ANOM) chart. Each data point in each chart is the average of the three readings in Table 1. The two groups for point density defined as A and B could not fit on the same ANOM chart. By looking between groups A and B, it is easy to see that the values with higher point density (A Group) have lower values and most values come down with lower scan speeds (from 5 to 1). The groups are significantly different. Since there are two predictor variables, one interaction should be checked. This interaction effect can be exploited or avoided as necessary only after it has been visualized. In the ANOM chart, the interaction can be visualised by observing the line between 3A and 2A and comparing it with the line between 3B and 2B. These are almost perpendicular, showing interaction is present. Numerical values (p values) of the statistical significance can be assigned by conducting an ANOVA test (as will be shown in 4.1).

So, in answer to the three initial questions:

Moving from higher (A) to lower (B) point density levels leads to significantly higher values for maximum individual pitch error.

Moving from higher (5) to lower (1) scan speeds levels leads to significantly lower values for maximum individual pitch error.

There is one point of interaction between scan speed and point density, and it occurs between levels 2A and 3A when compared to 2B and 3B.

In order to determine which values are more representative of the “true size” under study, further correlation work would be required by measuring the gear on an instrument with known uncertainties at the NGML. The purpose of this study is simply to determine if point density and scan speed (and their interaction) were statistically significant on the results obtained.

4. Orthogonal screening matrix

The ANOM / ANOR charts test whether the treatment means differ from the grand average or overall mean. When utilising an orthogonal array [8], it is possible to test whether multiple treatment means differ significantly from each other. To explore the effects of changing CMM parameters (or variables) on the measurement results, a factorial design matrix (or array) can be utilised. Since the output results from gear trials include many gear characteristics, the previous maximum individual pitch error (fpi) characteristic shall be considered.

4.1. Analysis via Factorial ANOVA

The matrix shown in Table 1 was generated in Minitab® statistical software. It was only necessary to specify the number of factors, the levels of factors, and the number of replications (in this case 3) for the matrix to be created. Normally, when completing trials in real time, it is recommended to do this in a random order and this order can be generated by the software. This was the case with the presented trials. Measurements were completed in the run order as shown and entered the data in the appropriate cell in the final column of Table 1. An analysis of variance (or ANOVA) test [8] was then conducted on the recorded data. The results of the analysis are shown in Table 2.

Table 2. Analysis of Variance Table for data in Table1

| Source | DF | Adj SS | Adj MS | F-Value | P-Value |
|--------------------------|----|---------|--------|---------|---------|
| Model | 11 | 14.5233 | 1.3203 | 10.26 | 0.000 |
| Blocks | 2 | 0.4847 | 0.2423 | 1.88 | 0.181 |
| Linear | 5 | 12.0773 | 2.4155 | 18.78 | 0.000 |
| Point Density | 1 | 6.1653 | 6.1653 | 47.93 | 0.000 |
| Scan Speed | 4 | 5.9120 | 1.4780 | 11.49 | 0.000 |
| 2-Way Interactions | 4 | 1.9613 | 0.4903 | 3.81 | 0.020 |
| Point Density*Scan Speed | 4 | 1.9613 | 0.4903 | 3.81 | 0.020 |
| Error | 18 | 2.3153 | 0.1286 | | |
| Total | 29 | 16.8387 | | | |

4.2. Observations

The results recorded in Table 1 were obtained from optical measurements when employing the HP-0 system. Analysis in Table 2 shows significant difference (p values < 0.05) for point density, scan speed, and their interaction confirming the findings of the ANOM and ANOR charts. At the time of writing the measurement trials from the optical and tactile studies are still ongoing and the results are far from complete, but the methodology shown demonstrates how results from various measurement methods could be compared. In order to see if the results of the optical and tactile results differ significantly, the graphical and numerical techniques outlined here would be utilised to make this determination. As previously stated, in order to see which methodology gave results closer to the true value, further correlation work would be required with the assistance of the NGML.

4.3. Study limitations

Due to initial hardware constraints, it was not possible to scan the full length of each gear tooth as would be required by the standard [1]. However, the methodology shown here provides a useful comparison between conventional CMM scanning and optical scanning over the same tooth area (as far in as can be achieved within the instrument constraints). This trial made use of the HPOAL sensor, and some results were inconsistent for some output parameters. The HPOAM optical probe may give more consistent results, and this will be the focus of future trials. DOE and ANOM / ANOR charts are able to investigate the effects of how changing any instrument parameters could be utilised to establish boundaries for uncertainty (both for individual sources and their interactions). Designed experiments could be applied to investigate various sources of instrument variation and sensitivity coefficients. DOE/DOX has advantages over the partial derivative method [9] since the various assumptions associated with ANOVA can (and always should) be tested using various *post hoc* analysis options as shown in Fig 4. These assumptions include that the “within group variation” is

homogeneous, no serial correlation is present between means and standard deviations, and that the residuals are normally distributed. These conditions were met during early trials.

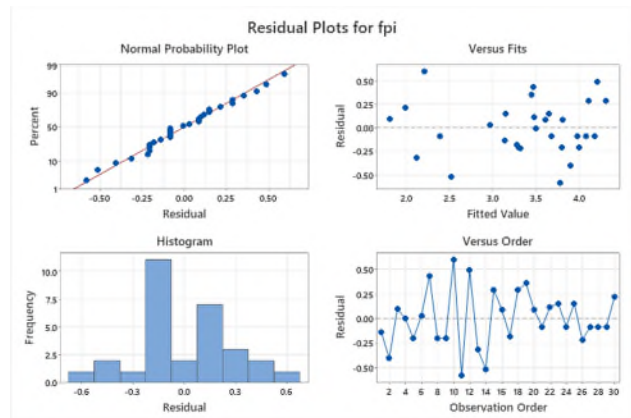


Fig 4. Plot of Residuals to test the assumptions of ANOVA

5. Conclusions

In this paper, the results of the optical gear measurement of individual gear pitch were reviewed. Firstly, the data sets were investigated utilising ANOM and ANOR charts, checking if the scanning speed and point density of the CMM sensor had an influence on the measurement results. It could be seen graphically that both predictor variables had an influence, and interaction was present. This means that both factors could be defined as significant sources of error and should be considered when developing any uncertainty budget [9]. The same data was reviewed in an orthogonal matrix/array, and with the use of modern statistical software it was simple to create the ANOVA table and confirm the graphical findings with numerical p values. All sources of variation (and interactions) not statistically significant (p > 0.05) could be removed from the uncertainty budget, and this would simplify any uncertainty calculation process since if the effects of any specific sources were not significant, then the uncertainty associated with that source could not be significant either. As point density and scan speed are significant, values for them should be defined when developing any part programs for the Coordinate measuring machine (CMM), and for any associated inspection plans.

Acknowledgments

We would like to thank the Manufacturing Technology Centre (MTC) and the UKRI Research England Development (RED) Fund for funding this work via the Midlands Centre for Data-Driven Metrology (MCDDM). We would also like to acknowledge the NGML for their ongoing support for this project.

References

1. BS ISO 1328-1-2013--[2022-03-18--03-04-03 PM]
2. PD ISO-TR 10064-1-2019--[2024-01-23--12-08-31 PM]
3. BS ISO 18653-2003--[2023-07-19--03-11-31 PM]
4. Flack D Good Practice Guide No. 41 CMM Measurement Strategies Issue 2
5. Flack D Good Practice Guide No. 43 CMM Probing Issue 2
6. 2008 BS 5702-2:2008 Guide to statistical process control (SPC) charts for variables-Part 2: Charts for individual values PERMISSION EXCEPT AS PERMITTED BY COPYRIGHT LAW BRITISH STANDARD
7. Donald J. Wheeler 1990 *Understanding Industrial Experimentation* Knoxville USA: SPC Press
8. R.J. Del Vecchio 1977 *Understanding Design of Experiments*
9. UKAS M3003:2022 The Expression of Uncertainty and Confidence in Measurement Edition 5